OL Organic Letters

pubs.acs.org/OrgLett Letter

Constructing Saturated Guanidinum Heterocycles by Cycloaddition of Amidinyliminium Ions with Indoles

Tyler K. Allred Michael B. Shagha Pan-Pan Chen Quan Tran K. N. Houk and Larry E. Overman

Cite This: *Org Lett* 2021 23 7618 7623 Read Online

CCESS | Metrics More | Article Recommendations | Supporting Information

ABSTRACT: We report that structurally complex guanidinium heterocycles can be prepared in one step by regio- and stereoselective [4 + 2]-cycloadditions of *N*-amidinyliminium ions with indoles or benzothiophene. In contrast to reactions of these heterodienes with alkenes, density functional theory (DFT) calculations show that these cycloadditions take place in a concerted asynchronous fashion. The [4 + 2]-cycloaddition of *N*-amidinyliminium ions (1,3-diaza-1,3-dienes) with indoles and benzothiophene are distinctive, as related [4 + 2]-cycloadditions of *N*-acyliminium ions (1-oxa-3-aza-1,3-dienes) are apparently unknown.

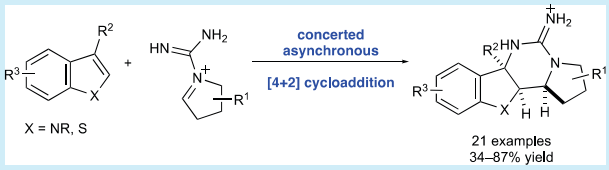

The guanidine functional group is found in a diverse array of drugs and potential therapeutics, re ecting its ability to form a variety of strong noncovalent interactions, such as hydrogen bonding and -stacking.[1] The anticancer agent pemetrexed (Alimta, **1**) exemplifies a class of therapeutic structures in which the guanidine is embedded in a polyheterocyclic unit.[2] Conversely, camostat mesylate (**2**), a drug for the treatment of chronic pancreatitis in Japan and currently under investigation as a potential therapy for SARS-CoV-2,[3] harbors an unsubstituted guanidine fragment (Figure 1). In addition, a wide variety of bioactive marine natural products contain guanidine units embedded in various

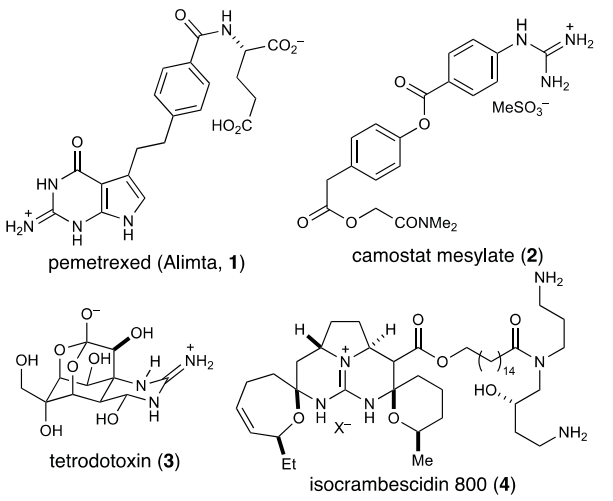

Figure 1. Selected drugs, drug candidates, and natural products containing a guanidinium group.

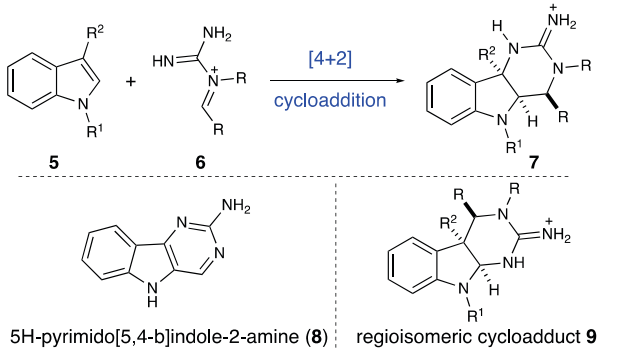

Figure 2. Preparation of guanidinium heterocycles **7** by cycloaddition of 3-substituted indoles **5** with *N*-amidinyliminium ions **6**.

Scheme 1. Cycloaddition to Form Tetracyclic Guanidinium Salts 12a b

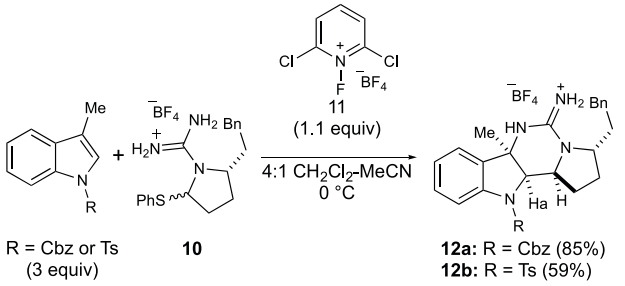

Received: August 23, 2021
Published: September 21, 2021

https://doi.org/10.1021/acs.orglett.1c02832
Org Lett 2021 23 7618 7623

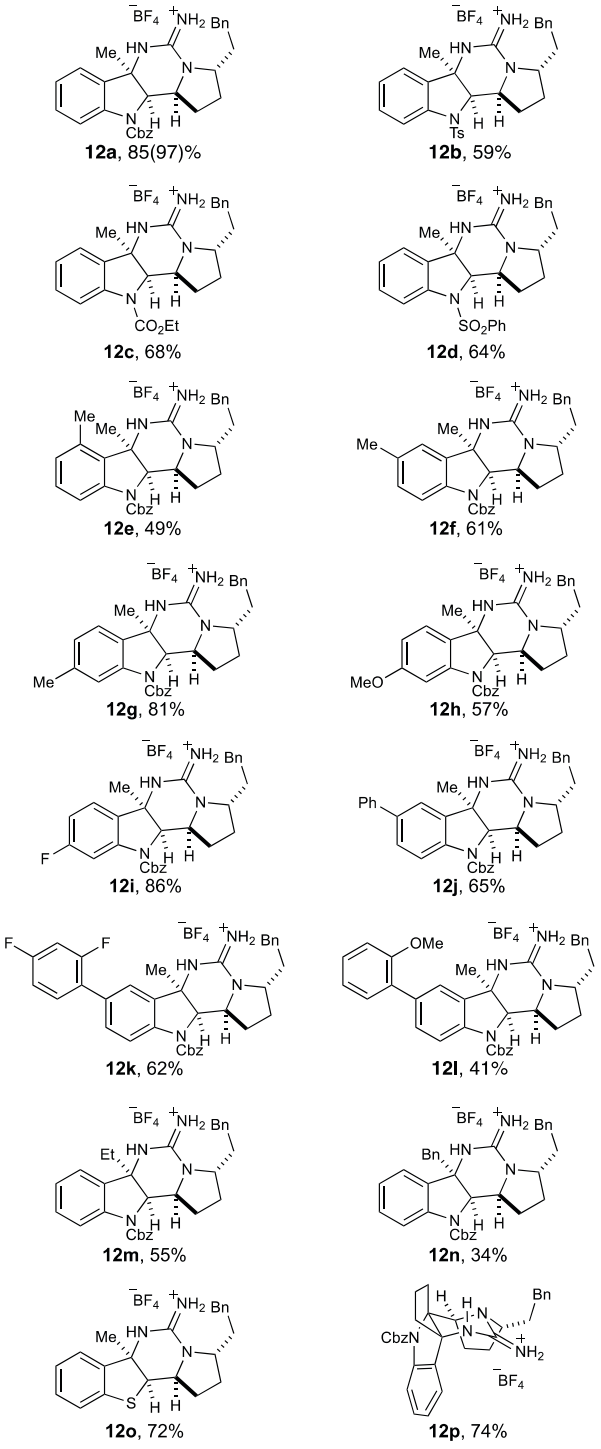

Figure 3. Scope of the cycloaddition of the amidinyl iminium ion derived from phenylthio precursor **9** and indoles or benzothiophene. Reactions were conducted under the conditions depicted in Scheme 1. The yield of **12a** was 97 in a reaction conducted at the 1 mmol scale. Several products contained a small amount of an inseparable byproduct, which could be a regio- or stereoisomer.

polycyclic scaffolds, as exemplified by tetrodotoxin (**3**) and isocrambescidin 800 (**4**).[1,4]

Herein we report that guanidinium heterocycles, exemplified by **7**, featuring a dihydroindole motif can be prepared by cycloaddition of *N*-amidinyliminium ions with 3-substituted

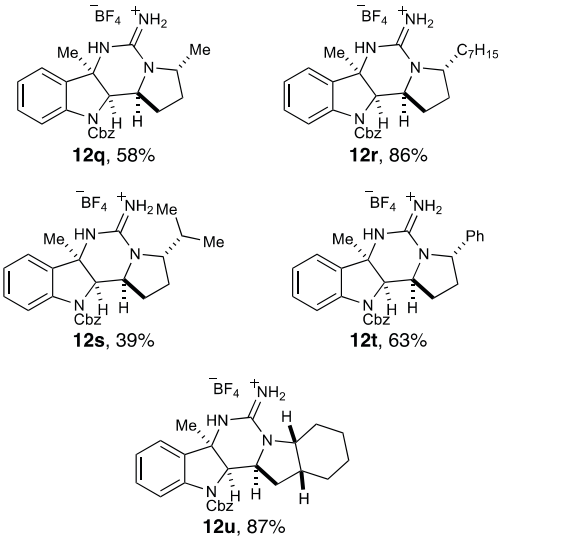

Figure 4. Scope of the cycloaddition of 1-(benzyloxycarbonyl)-3-methylindole with several novel *N*-amidinyliminium ions derived from phenylthio precursors. Reactions were conducted under the conditions depicted in Scheme 1.

indoles (Figure 2). Polycyclic guanidinium structures of this type are of interest as a result of the diverse pharmacological activities reported for unsaturated analogues **8**[5] and the recent realization that increasing the fraction of sp^3 and chiral centers in drug candidates improves clinical success.[6] The cycloadditions of indoles with *N*-amidinyliminium ions reported here represent extremely rare examples of the bimolecular [4 + 2] cycloaddition of indoles with hetero-1,3-dienes.[7]

The chemistry of iminium ions harboring an *N*-amidinyl substituent is largely unexplored.[8] We first encountered these iminium ion variants as intermediates in tethered Biginelli reactions.[4b] Subsequently, we developed a method to generate these electrophiles under aprotic conditions from the reaction of α-(thiophenyl)guanidinium ions with $Cu(OTf)_2$ and studied their reaction with electron-rich alkenes.[9] To further explore the reactivity of *N*-amidinyliminium ions, we recently investigated their reactivity with indoles. We began by examining the reaction of several indoles with *N*-amidinyliminium ion precursor **10** using the thiophilic reagent 2,6-dichloro-1- uoropyridinium tetra uoroborate (**11**),[10] which had performed exceptionally well in recent studies of the cyclocondensation reaction of **10** with styrenes (Scheme 1).[11] Although 1-methylindole and 1,3-dimethylindole gave complex mixtures of reaction products, 3-methylindoles harboring a Cbz or Ts substituent on nitrogen provided one major cycloadduct **12** on exposure to **10** and 1 equiv of the *N*- uoropyridinium salt **11** at 0 °C in CH_2Cl_2 (or mixtures of acetonitrile and CH_2Cl_2). Additional optimization experiments showed that the reaction of 3 equiv of the indole, 1 equiv of iminium ion precursor **10**, and 1.1 equiv of **11** at 0 °C in a 4/1 CH_2Cl_2/MeCN solvent mixture in the presence of 4 Å molecular sieves gave cycloadducts **12a**,**b** with high diastereoselectivity in 85 97 and 59 yields, respectively (Figure 3). The structure of these cycloadducts was originally assigned on the basis of NMR spectra. Particularly diagnostic were the downfield resonance for the fully substituted benzylic carbon (**12a**, 61.9 ppm; **12b**, 63.7 ppm) and the signal for Ha, which appeared at 4.82 and 4.28 ppm as a clean doublet (J = 5.3 and 4.5 Hz) for **12a**,**b**, respectively. These data rule out the alternate regioisomeric structure **9**. The relative configurational assign-

https://doi.org/10.1021/acs.orglett.1c02832
Org Lett 2021 23 7618 7623

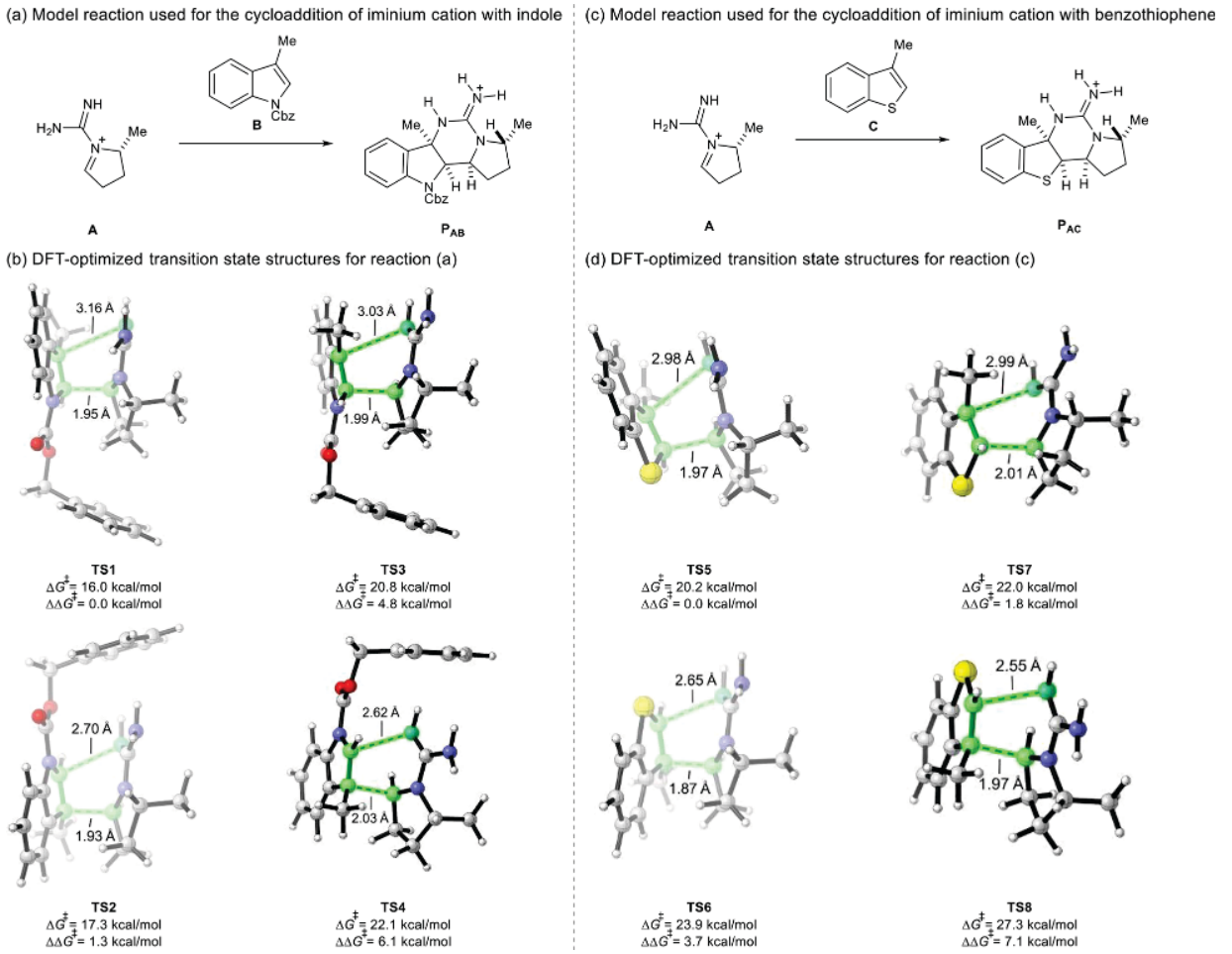

Figure 5. Model reactions (a, c) studied computationally. DFT-optimized transition state structures (b, d). The energy zero is the separate reactants.

ment to cycloadducts **12**, which was originally proposed on the expectation of *endo* cycloaddition from the face opposite the phenethyl substituent, was subsequently confirmed by a single-crystal X-ray analysis of product **12j** bearing a phenyl substituent on the aromatic ring (see below).

The results of our survey of the cycloaddition of the *N*-amidinyliminium ion derived from thioaminal precursor **10** with various substituted indoles are summarized in Figure 3. Useful yields were obtained when the indole nitrogen was protected with either a carbamate or sulfonyl substituent. Substitution at C-5 or C-6 of the indole precursor was well tolerated (formation of **12f i**). These polar guanidinium products are difficult to isolate in pure form; therefore, differences in yield of 10 20 undoubtedly re ect these challenges. Nonetheless, the significantly lower yields observed in forming **12e**,**n** and the lack of reactivity of 3-isopropylindole derivatives (see the Supporting Information) likely re ects a steric impediment to creating the fully substituted benzylic C N σ-bond. Indoles harboring electron-withdrawing substituents at C-3 or C-5, or a siloxymethyl substituent at C-3, were not successful reaction partners (see the Supporting Information). It is notable that benzothiophene participated well in the cycloaddition reaction, giving rise to cycloadduct **12o** in 72 yield. In addition, the structurally intricate bridged pentacycle **12p** could be accessed by utilizing a 1,2,3,4-tetrahydrocyclopent[*b*]indole derivative in the *N*-amidinyliminium ion cycloaddition.

We then explored this cycloaddition method with 1-(benzyloxycarbonyl)-3-methylindole and several alternate *N*-amidinyliminium ion precursors (Figure 4). Truncation of the phenethyl substituent is well tolerated, as illustrated by **12q**. There is a diminished yield for adduct **12s**, which is not surprising considering the effect that steric in uences played in our examination of the indole scope (see the Supporting Information). In addition, more complex *N*-amidinyliminium ion precursors could be utilized, as exemplified by the formation of adduct **12u**.

Intrigued by the observed regio- and stereoselectivity of this type of cycloaddition reaction, we undertook density functional theory (DFT) calculations to gain further insight into the underlying mechanism.[12 15] On the basis of the experimental results, the model reactions shown in Figure 5a,c were used for the computational study. Figure 5b shows DFT-optimized transition state (TS) structures for the cycloaddition of **A** (iminium cation) with **B** (indole substrate). We calculated four possible TSs. The competition between **TS1** and **TS2** determines the regioselectivity, while the energy difference between **TS1** and **TS3** determines the stereoselectivity. **TS1** is the most favorable and leads to the experimentally observed product. We also calculated four possible transition states (Figure 5d) for the cycloaddition of **A** (iminium cation) with **C** (benzothiophene substrate) on the basis of the model reaction shown in Figure 5c.

https://doi.org/10.1021/acs.orglett.1c02832
Org Lett 2021 23 7618 7623

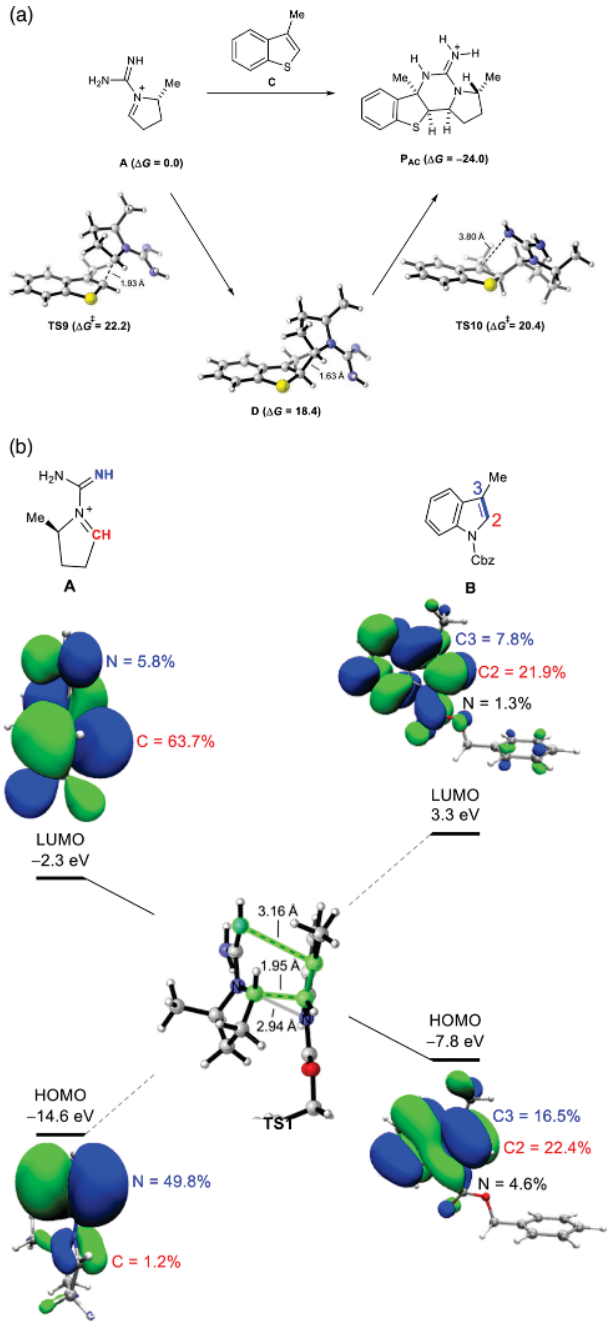

Figure 6. (a) Stepwise cycloaddition mechanism. Free energies are given in kcal/mol. (b) Orbital interaction diagram for the cycloaddition of **A** and **B**. Percentages given are the fraction of electron density at that position in that orbital.

The competition between **TS5** and **TS6** determines the regioselectivity, while the energy difference between **TS5** and **TS7** determines the stereoselectivity. Of the four transition states studied, **TS5** is the most favorable and generates the experimentally observed product (Figure 5d). Our computational results are consistent with the experimental observations. The calculated transition states shown in Figure 5b,d are highly asynchronous, but intrinsic reaction coordinate (IRC) calculations confirm the concerted nature of these transition states.

In addition to the concerted mechanism, we also studied the possibility of a stepwise pathway. As shown in Figure 6a, for the cycloaddition of **A** (iminium cation) with **C** (benzothiophene substrate), a stepwise mechanism occurs via **TS9** to form the first C C bond, and the barrier is 22.2 kcal/mol. The energy of the resulting stepwise intermediate, **D**, is 18.4 kcal/mol. Next, the second C N bond formation occurs via **TS10**, which has a free energy of 20.4 kcal/mol. Overall, the rate-limiting step for the stepwise mechanism is the first C C bond formation, and the barrier is 22.2 kcal/mol (via **TS9**). Thus, the stepwise mechanism is less favorable in comparison to the concerted mechanism, in which the overall barrier is 20.2 kcal/mol (via **TS5**, Figure 5d).

To understand the origins of regioselectivity for the cycloaddition of **A** with **B**, we studied the orbital interaction between the reactants. The orbital interaction diagrams shown in Figure 6b suggest that the dominant interaction is from the HOMO of **B** to the LUMO of **A**, which produces not only the primary orbital interaction (highlighted in green) but also the favorable secondary orbital interaction (SOI, gray line) between nitrogen and nitrogen. The difference in nucleophilicity between C2 and C3 (orbital coefficients for C2 and C3 in HOMO) of **B** determines the regioselectivity, making **TS1** more favorable than **TS2**. Similar orbital interactions control the cycloaddition of **A** with **C** (Figure S1).

We also explored the origins of stereoselectivity for these cycloadditions. The *endo* **TS1** is favored by 4.8 kcal/mol versus the *exo* **TS3**. The *endo* TSs are favored by 1.8 4.8 kcal/mol for all four cycloadditions depicted in Figure 6b. Secondary orbital interactions and stabilizing electrostatic interactions[16] between the systems of **B** and **C** and the cationic diene, **A**, favor the *endo* transition state in every case (Figure 6b and Figure S1).

In summary, complex guanidinium heterocycles harboring fragment **7** can be prepared by [4 + 2]-cycloaddition of *N*-amidinyliminium ions with indoles. This reactivity of *N*-amidinyliminum ions appear to be unique, as related [4 + 2]-cycloadditions of *N*-acyliminium ions are apparently unknown.[17] In contrast to reactions of *N*-amidinyliminium ions with alkenes,[9] the [4 + 2]-cycloadditions of these cationic heterodienes with indoles and benzothiophenes ions occur in a concerted, asynchronous fashion. The high regio- and stereoselectivity of these concerted cycloadditions are reproduced by DFT calculations and explained by a simple FMO model. This cycloaddition approach should allow the diverse pharmacological activity of heterocycles containing the 5*H*-pyrimidino-[5,4-*b*]indole-2-amine (**8**) moiety to be explored with analogues having a three-dimensional structure.[6]

ASSOCIATED CONTENT

Supporting Information

The Supporting Information is available free of charge at https://pubs.acs.org/doi/10.1021/acs.orglett.1c02832.

Reaction optimization, experimental procedures, computational methods, characterization data for all new compounds, and X-ray analysis of **12j** (PDF)

Accession Codes

CCDC 2102746 contains the supplementary crystallographic data for this paper. These data can be obtained free of charge via www.ccdc.cam.ac.uk/data_request/cif, or by emailing data_request@ccdc.cam.ac.uk, or by contacting The Cambridge Crystallographic Data Centre, 12 Union Road, Cambridge CB2 1EZ, UK; fax: +44 1223 336033.

https://doi.org/10.1021/acs.orglett.1c02832
Org Lett 2021 23 7618 7623

AUTHOR INFORMATION

Corresponding Authors

K. N. Houk *Department of Chemistry Biochemistry University of California Los Angeles California 90095-1569 United States;* orcid.org/0000-0002-8387-5261; Email: houk@chem.ucla.edu

Larry E. Overman *Department of Chemistry University of California Irvine California 92697-2025 United States;* orcid.org/0000-0001-9462-0195; Email: leoverma@uci.edu

Authors

Tyler K. Allred *Department of Chemistry University of California Irvine California 92697-2025 United States*

Michael B. Shagha *Department of Chemistry University of California Irvine California 92697-2025 United States*

Pan Pan Chen *Department of Chemistry Biochemistry University of California Los Angeles California 90095-1569 United States*

Quan Tran *Department of Chemistry Biochemistry University of California Los Angeles California 90095-1569 United States*

Complete contact information is available at: https://pubs.acs.org/10.1021/acs.orglett.1c02832

Author Contributions

L.E.O., K.N.H., and M.B.S. designed the research. Laboratory experimentation and data analysis were conducted by T.K.A. and M.B.S. Computational studies were conducted by P.-P.C. and Q.T. All authors analyzed the results and wrote and reviewed the article.

Notes

The authors declare no competing financial interest.

ACKNOWLEDGMENTS

This work was generously supported by the National Science Foundation (CHE-1764328 to K.N.H. and CHE-1661612 to L.E.O.). P.-P.C. is grateful for support from Zhejiang University, Hangzhou, China and M.B.S. for support from Eli Lilly and Co. Calculations were performed on the IDRE Hoffman2 cluster at the University of California, Los Angeles. We thank Dr. Peng Zhao, University of California, Irvine, for early experimental contributions to this study.

REFERENCES

(1) For reviews, see: (a) Greenhill, J. V.; Lue, P. Amidines and guanidines in medicinal chemistry. *Prog. Med. Chem.* **1993**, *30*, 203 326. (b) Khalaf, M.; Zageer, D.; Hussain, Z.; Adil, H.; Mohammed, S.; Yousif, E. Z. Guanidine group: definition and pharmaceutical applications. *J. Pharm. Biol. Chem. Sci.* **2016**, *7*, 1026 1031. (c) Berlinck, G. S.; Bernardi, D. I.; Fill, T.; Fernandes, A. A. G.; Juberg, I. D. The chemistry and biology of guanidine secondary metabolites. *Nat. Prod. Rep.* **2021**, *38*, 586 667 and earlier reviews in this series.

(2) Taylor, E. C.. In *Successful Drug Discovery*; Fischer, J., Rotella, D. P., Eds.; Wiley-VCH: 2015; pp 157 180.

(3) Hoffmann, M.; Hofmann-Winkler, H.; Smith, J. C.; Kruger, N.; Arora, P.; Sørensen, L. K.; Søgaard, O. S.; Hasselstrøm, J. B.; Winkler, M.; Hempel, T.; Raich, L.; Olsson, S.; Danov, O.; Jonigk, D.; Yamazoe, T.; Yamatsuta, K.; Mizuno, H.; Ludwig, S.; Noe, F.; Kjolby, M.; Braun, A.; Sheltzer, J. M.; Pohlmann, S. Camostat mesylate inhibits SARS-CoV-2 activation by TMPRSS2-related proteases and its metabolite GBPA exerts antiviral activity. *EBioMedicine* **2021**, *65*, 103255.

(4) For selected reviews, see: (a) Reference 1c. (b) Aron, Z. D.; Overman, L. E. The tethered Biginelli condensation in natural product synthesis. *Chem. Commun.* **2004**, 253 265. (c) Shi, Y.; Pierce, J. G. Structure, synthesis and biological properties of the pentacyclic guanidinium alkaloids. *Bioorg. Med. Chem.* **2017**, *25*, 2817 2824.

(5) For two selected examples, see the following. Antitumor agents: (a) Gasparoli, L.; D Amico, M.; Masselli, M.; Pillozzi, S.; Caves, R.; Khuwaileh, R.; Tiedke, W.; Mugridge, K.; Pratesi, A.; Mitcheson, J. S.; Basso, G.; Becchetti, A.; Arcangeli, A. New pyrimidoindole compound CD-160130 preferentially inhibits the KV11.1B isoform and produces antileukemic effects without cardiotoxicity. *Mol. Pharmacol.* **2015**, *87*, 183 196. Neuroprotective agents: (b) Wang, G.; Han, T.; Nijhawan, D.; Theodoropoulos, P.; Naidoo, J.; Yadavalli, S.; Mirzaei, H.; Pieper, A. A.; Ready, J. M.; McKnight, S. L. P7C3 neuroprotective chemicals function by activating the rate-limiting enzyme in NAD salvage. *Cell* **2014**, *158*, 1324 1334.

(6) Lovering, F.; Bikker, J.; Humblet, C. Escape from flatland: increasing saturation as an approach to improving clinical success. *J. Med. Chem.* **2009**, *52*, 6752 6756.

(7) The only other intermolecular examples that we are aware of involve the cycloaddition of azoalkenes (1,2-diaza-1,3-dienes): (a) Clarke, S. J.; Davies, D. E.; Gilchrist, T. L. Competing [4 + 2] and [3 + 2] cycloaddition in the reactions of nucleophilic olefins with ethyl 3-(toluene-*p*-sulphonylazo)but-2-enoate. *J. Chem. Soc. Perkin Trans. 1* **1983**, 1803 1807. (b) Tong, M.-C.; Chen, X.; Li, J.; Huang, R.; Tao, H.; Wang, C.-J. Catalytic asymmetric synthesis of [2,3]-fused indoline heterocycles through inverse-electron-demand aza-Diels Alder reaction of indoles with azoalkenes. *Angew. Chem. Int. Ed.* **2014**, *53*, 4680 4684. (c) Ciccolini, C.; Mari, G.; Gatti, F. G.; Gatti, G.; Giorgi, G.; Mantellini, F.; Favi, G. Synthesis of polycyclic fused indoline scaffolds through a substrate-guided reactivity switch. *J. Org. Chem.* **2020**, *85*, 11409 11425. For a recent example of reactions promoted by electrochemical activation, see: (d) Song, C.; Liu, K.; Jiang, X.; Dong, X.; Weng, Y.; Chiang, C.-W.; Lei, A. Electrooxidation enables selective dehydrogenative [4 + 2] annulation between indole derivatives. *Angew. Chem. Int. Ed.* **2020**, *59*, 7193 7197.

(8) In addition to our investigations, *N*-amidinyliminium ions have been encountered occasionally as intermediates in synthetic routes to pyrrole-imidazole alkaloids. See, for example: (a) O Malley, D. P.; Li, K.; Maue, M.; Zografos, A. L.; Baran, P. S. Total synthesis of dimeric pyrrole imidazole alkaloids: sceptrin, ageliferin, nagelamide E, oxysceptrin, nakamuric acid, and the axinellamine carbon skeleton. *J. Am. Chem. Soc.* **2007**, *129*, 4762 4775. (b) Ding, H.; Roberts, A. G.; Harran, P. G. Total synthesis of ageliferin *via* acyl *N*-amidinyliminium ion rearrangement. *Chem. Sci.* **2013**, *4*, 303 306.

(9) Wolfe, J. P.; Overman, L. E. Synthesis of polycyclic guanidines by cyclocondensation reactions of *N*-amidinyliminium ions. *J. Org. Chem.* **2001**, *66*, 3167 3175.

(10) Tsukamoto, H.; Kondo, Y. 1-Fluoropyridinium triflates: versatile reagents for transformation of thioglycoside into *O*-glycoside, glycosyl azide and sulfoxide. *Tetrahedron Lett.* **2003**, *44*, 5247 5249.

(11) Shaghafi, M. B.; Barrett, D. G.; Willard, F. S.; Overman, L. E. The insulin secretory action of novel polycyclic guanidines: discovery through open innovation phenotypic screening, and exploration of structure-activity relationships. *Bioorg. Med. Chem. Lett.* **2014**, *24*, 1031 1036.

(12) Geometry optimizations of all intermediates and transition states were performed at the B3LYP13[13] level of theory with the def2-SVP14 basis set,[14] including solvation energy corrections and Grimme s D3 dispersion corrections.[15] Additional computational details are included in the Supporting Information.

(13) Becke, A. D. A. New mixing of Hartree-Fock and local density-functional theories. *J. Chem. Phys.* **1993**, *98*, 5648 5652.

(14) Weigend, F.; Ahlrichs, R. Balanced basis sets of split valence, triple zeta valence and quadruple zeta valence quality for H to Rn: Design and assessment of accuracy. *Phys. Chem. Chem. Phys.* **2005**, *7*, 3297 3305.

(15) Grimme, S.; Antony, J.; Ehrlich, S.; Krieg, H. A consistent and accurate ab initio parametrization of density functional dispersion

correction (DFT-D) for the 94 elements H-Pu. *J. Chem. Phys.* **2010**, *132*, 154104.
(16) Woodward, R. B.; Baer, H. Studies on diene-addition reactions. II. The reaction of 6,6-pentamethylenefulvene with maleic anhydride. *J. Am. Chem. Soc.* **1944**, *66*, 645 649.
(17) (a) Examples have not been found in comprehensive reviews of the chemistry of *N*-acyliminium ions, including a recent review of their use to form diverse heterocyclic skeletons. See: Wu, P.; Nielson, T. E. Scaffold diversity from *N*-acyliminium ions. *Chem. Rev.* **2017**, *117*, 7811 7856. (b) No examples have been found from generic reaction searches in SciFinder nor from structural searches in SciFinder for products that would result from [4 + 2]-cycloaddition of these 1-oxa-3-aza-1,3-dienes with indoles or benzothiophene.

https://doi.org/10.1021/acs.orglett.1c02832
Org Lett 2021 23 7618 7623